JJEE
Volume 5, Number 4, 2019
Pages 202-221
Jordan Journal of Electrical Engineering
ISSN (Print): 2409-9600, ISSN (Online): 2409-9619

Comparative Analysis of Induction Motor and Interior Permanent Magnet Synchronous Motor in Electric Vehicles with Fuzzy Logic Speed Control

Ahmad Y. Abu-Ghazal[1*], Qazem M. Jaber[2]

[1, 2] Department of Mechatronics Engineering, Al-Balqa Applied University, Amman, Jordan
E-mail: ahmadyaser1991@yahoo.com

Received: September 2, 2019 *Revised: October 4, 2019* *Accepted: October 12, 2019*

***Abstract*—** Selection of electric motors and designing of efficient motor drives are important issues in the manufacturing of electric vehicle's traction system, especially with the highly competitive electric vehicles' market. Many electric motors can be used to drive electric vehicles, but the induction motor (IM) and the interior permanent magnet synchronous motor (IPMSM) are the dominant ones. This paper introduces a dynamic comparative analysis of the IM and the IPMSM in electric vehicles applications. To conduct this analysis, two identical IM and IPMSM have been selected and two motor drives have been built using field oriented control (FOC) techniques in Simulink software. The motors were used to drive identical vehicle body models with a fuzzy logic controller used to control the vehicle's speed. Both motors were compared mainly in terms of the speed and the torque responses with and without vehicle body load. The results showed a convergent performance between both systems; however, the IM-driven vehicle model has a little faster response compared to the IPMSM-driven one, whereas the latter has a higher torque ripple compared to the IM drive.

***Keywords*—** Electric vehicles; Induction motor; Interior permanent magnet synchronous motor; Fuzzy logic control; Field oriented control; Simulink.

1. INTRODUCTION

The electric motor is the main active component in electric vehicles; it converts electric energy stored in the vehicle battery into mechanical energy, which moves the vehicle. Also, it works as a generator during the regenerative braking mode, which converts the mechanical energy generated from braking into electrical energy, and stores it back in the battery. The main electric motors used in electric vehicles are DC motors, induction motors (IM), permanent magnet synchronous motors (PMSM) and switched reluctance motors (SRM) [1]. According to the global electric vehicle sales in 2018 [2], the most sold models were Tesla Model 3 (which is an American-made car), BAIC EC-series (which is a Chinese-made car), and Nissan Leaf (which is a Japanese-made car) . The electric motor type used in Tesla car is the induction motor (IM) while the permanent magnet synchronous motor PMSM is used in BAIC and Nissan leaf cars [3].

The induction motor provides multiple advantages such as simple and robust design, wide speed range and low cost because it does not contain rare earth magnets.

The permanent magnet synchronous motors are classified into two categories based on the position of the magnets within the rotor: the surface permanent magnet synchronous motors (SPMSM), and the interior permanent magnet synchronous motors (IPMSM) as shown in Fig. 1 [4].

* Corresponding author

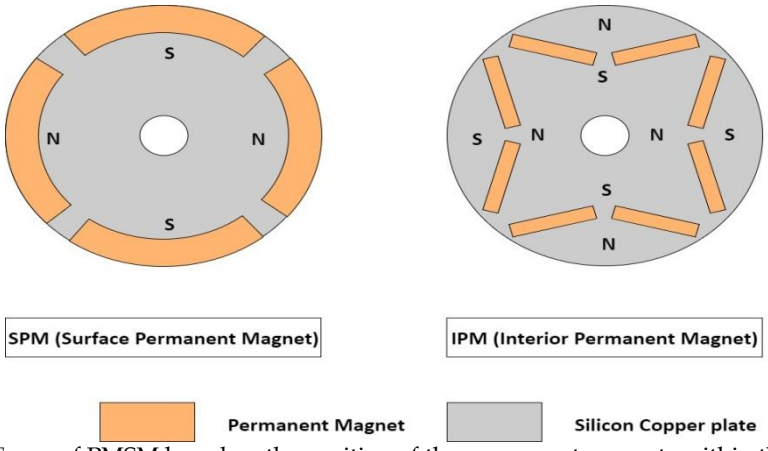

Fig. 1. Types of PMSM based on the position of the permanent magnets within the rotor.

The IPMSM is more preferred in electric vehicles applications due to its mechanical robustness, overload capability, high-speed operation, and many other advantages [5]. Fig. 2 shows the IPMSM type rotor used in Nissan leaf [6].

Fig. 2. Nissan leaf IPMSM rotor.

Induction motors and interior permanent magnet synchronous motors are successfully used in electric vehicles, so the advantages of using each motor over the other in electric vehicle traction systems need to be further examined.

Many researches have conducted comparative studies between the IM and the IPMSM motors. In [7], a comparative study on fuzzy logic vector control of an IM and a PMSM for hybrid/electric vehicle traction applications using MATLAB/Simulink was presented. The same controller was used for the two motor drives to provide a comparison between the performance of the two motors, one using a fuzzy logic controller and the other using a proportional–integral–derivative controller (PID) for both drives. But the motors used were not at the same power, voltage, current and speed ratings, so the terms were not common between the two drives. In [8], a comparison was conducted between Toyota Prius 2010 IPMSM and IM that was designed with the same stator outer diameter and stack length as the IPMSM in order to achieve a fair comparison. The performance of the two motors was compared by the torque capability, torque/power-speed characteristics, power factor, torque ripple and efficiency. The material cost for both motors was also evaluated.

Other researchers have compared the IM and the IPMSM in terms of the design of motors themselves and their performance by finite element analysis (FEA) methods. In [9], the IM, SPMSM, and IPMSM were compared. The common specifications among the compared motors' designs were outer dimensions of the active parts (stack diameter and length), inverter size (maximum voltage and maximum current), cooling method, and continuous power at the maximum motor speed. Then, a comparison was conducted on the motors' designs using FEA in terms of output power, efficiency, energy loss, and overload capability. The results showed that the IPMSM has the best performance among the compared motors.

This paper provides a dynamic comparison between the IM and IPMSM. The comparison is made using Simulink platform; and motors with the same power, torque and ratings are employed. Also the motors are attached to the same vehicle body model, which was designed to meet the motors' specifications. The used electric vehicle's drive system starts by a speed command generated by the user; and the vehicle speed is regulated by a fuzzy logic controller (FLC), which provides a torque signal to the field-oriented controller (FOC) that drives the motor through a space vector pulse-width modulator (SVPWM).

The SVPWM converts the currents command from the FOC to voltage commands by proportional–integral (PI) regulators; then the voltage command is converted to a reference voltage space vector with a known magnitude and angle. According to the magnitude and angle of the reference voltage space vector, gates of the inverter are fired at part-time basis to produce the desired output voltage of the inverter. For further theory about the SVPWM, refer to [10].

The inverter converts the DC battery voltage to AC three phase voltage on the motor side. The electric motor drives the vehicle body model through a gearbox. All blocks are common between the IM and IPMSM-driven electric vehicles modes except the FOC controller since each motor type has its own FOC method. Fig. 3 shows the block diagram of the electric vehicle drive system components and the signals between them. These strict terms ensure a fair comparison between the IM and IPMSM when used in electric vehicles.

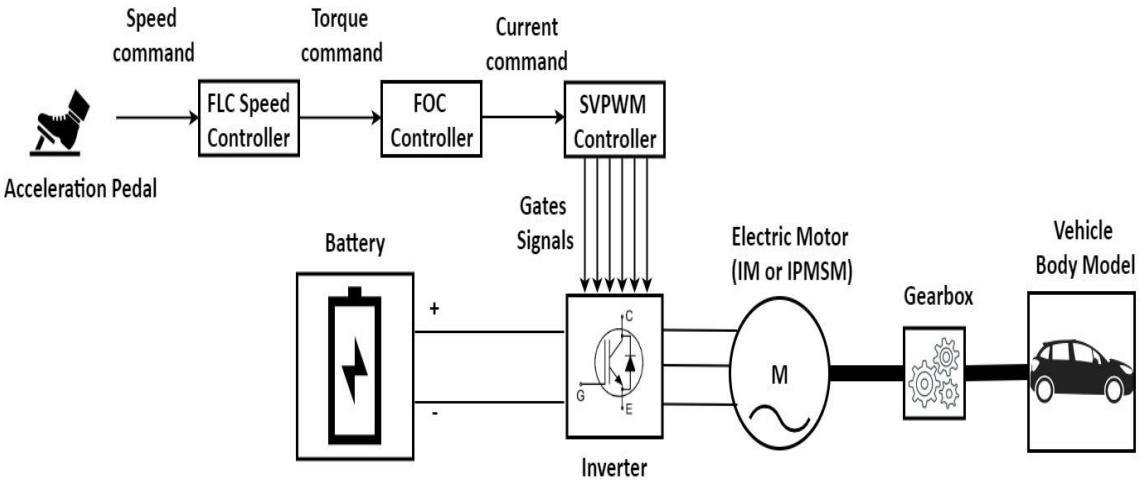

Fig. 3. Block diagram of the electric vehicle drive system.

The comparison is oriented towards the dynamic response of the motors, which includes the speed, torque, and output power responses. Also the motors' drives were tested on a standard driving cycle called extra urban driving cycle (EUDC) for low power vehicles.

2. MOTORS PARAMETERS

Intensive efforts have been done to find identical IM and IPMSM to make sure that the comparison between them will be reasonable. Two motors with 40 HP (about 30 kW) rated power have been found; and the parameters for each motor are very close to each other as shown in the following section.

2.1. IM Parameters

Usually, the manufacturer's catalogues do not contain the equivalent circuit parameters of the IM, which the Simulink model needs. In fact, the catalogues mainly mention the parameters that are useful for the motor operation conditions. The catalogue data of the used IM are listed in Table 1 [11].

Table 1. Catalogue data of the selected IM.

Parameter		Value
Output [kW]		30
Rated line voltage [V]		460
Rated frequency [Hz]		60
Full load current [A]		47.1
Full load torque [N.m]		158.631
Locked rotor torque [N.m]		348.988
Break-down torque [N.m]		380.714
Rotor inertia [Kg.m^2]		0.387
Poles numbers		4
Rated speed [rpm]		1775
Efficiency [% of full load]	50 %	93.9
	75%	94.1
	100%	94.1
Power factor [% of full load]	50 %	0.72
	75%	0.8
	100%	0.85

A mathematical model presented in [12] is used to find the parameters of the IM equivalent circuit that uses the full load speed, rated torque, starting torque, efficiency, and power factor values at the rated load. To calculate the stator resistance and the leakage reactance, 75% and 50% of the rated load is used. Rotor resistance and leakage reactance refer to stator and the magnetizing reactance and resistance.

The equations listed in [12] are applied on the values listed in Table 1 to find the values of the IM equivalent circuit parameters that will be used in the simulation model. The parameters of the IM are listed in Table 2.

Table 2. IM equivalent circuit's calculated parameters.

Parameter	Symbol	Value [Ω]
Stator resistance	R_s	0.11122
Stator leakage reactance	X_{ls}	0.13
Magnetizing reactance	X_m	17.11
Magnetizing resistance	R_m	847.070
Rotor resistance referred to stator	R_r	0.08533
Rotor leakage reactance referred to stator	X_{lr}	0.13

2.2. IPMSM Parameters

The catalogue data of the selected IPMSM are shown in Table 3 [13], in which L_d and L_q are the direct-axis and quadrature-axis magnetizing inductances, respectively.

Table 3. Catalogue data of the selected IPMSM.

Parameter	Value
Rated HP	40
Full load torque [N.m]	158.22
Rated line voltage [V]	460
Full load current [A]	45.5
Rated frequency [Hz]	120
Poles number	8
Rated speed [rpm]	1800
Full load efficiency [%]	95.4
Resistance per phase [Ω]	0.06
L_d [mH]	4.420
L_q [mH]	6.970
L_q : L_d ratio	1.6
Rotor inertia [kg.m^2]	0.304

Here, the data needed for Simulink model of the IPMSM are listed except the torque constant (torque per peak ampere) and the flux linkage established by magnets in [Wb]. For the torque constant, it can be calculated directly from the full load torque and the full load current in the catalogue data (158.63 N.m/(45.5*√2) A= 2.465 N.m/A).

The flux linkage established by magnets was estimated by simulating the motor model with the above parameters and by using the torque equation of the IPMSM, which equals 0.4108 V.s.

In the Simulink model of the IPMSM, the user can specify the torque constant or the flux linkage established by magnets, but not both; and the flux linkage established by magnets' parameters was used.

2.3. Motors Parameters Summary

The main parameters of the two motors are shown in Table 4. The friction factor of both motors was set to be equal to 0.005 N.m.s, so it can be noticed that the parameters are very close to ensure a fair comparison.

Table 4. Summary of IM and PMSM parameters.

Parameter	Motor	
	IM	IPMSM
Rated power [HP]	40	40
Rated torque [N.m]	158.63	158.22
Rated speed [rpm]	1775	1800
Rated line voltage [V]	460	460
Full load current [A]	47.1	45.5
Rotor inertia [kg.m^2]	0.387	0.304

3. VEHICLE BODY MODEL

The Simulink models of the vehicle's body and the tires, which were used in the simulation, are shown in Fig. 4. The vehicle's body model is connected to the motor as a mechanical rotational port, which treats the output of the motor as a real shaft with its own speed and torque. The driveshaft is connected to a gearbox block for torque matching and then to the tires by front and rear differentials. As shown, the incline angle of the road and wind speed could be specified in the vehicle's body block.

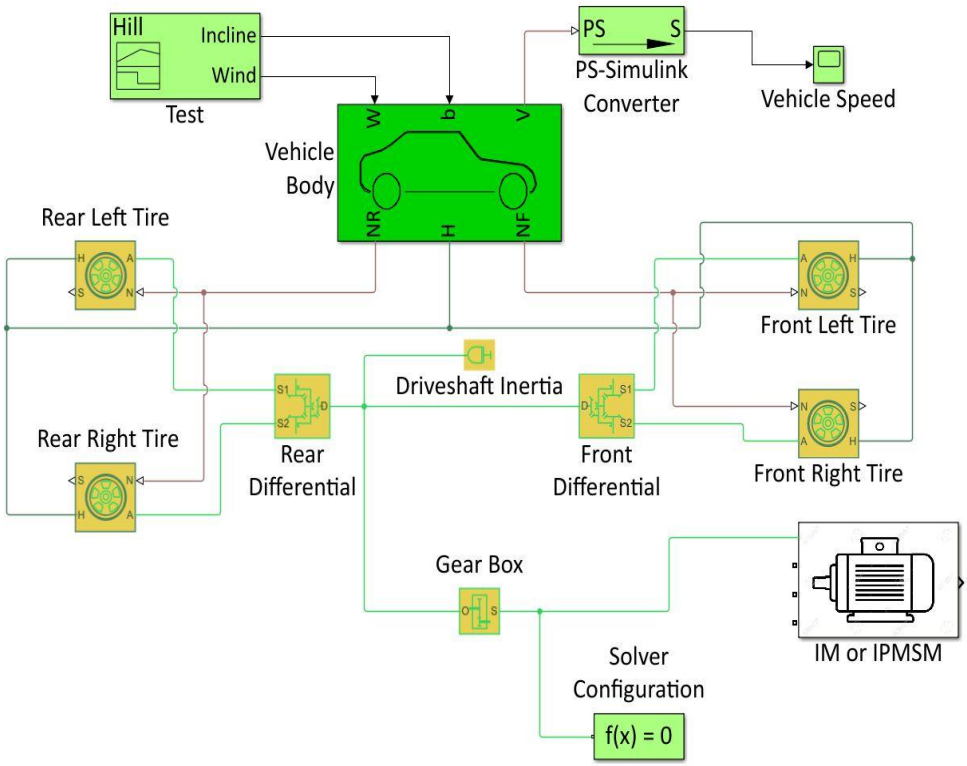

Fig. 4. Simulink model of the vehicle's body with tires.

The vehicle's body parameters exhibited in Table 5 are the same as those of the Nissan Leaf car, which are listed in [14]. Air density is the standard air density at sea level as listed in [15]. The gear ratio and vehicle mass are calculated using equations described in [16, 17] to make the vehicle's acceleration convenient.

Table 5. Parameters of vehicle's body.

Parameter	Value
Vehicle effective frontal area [m^2]	2.29
Vehicle mass [Kg]	600
Gear ratio	3.14
Wheel radius [m]	0.3
Aerodynamic drag coefficient	0.28
Rolling resistance coefficient	0.007
Air density [Kg/m^3]	1.225

4. THE IM DRIVE

4.1. IM Mathematical Model

The equations of the synchronously rotating reference frame voltages in the stator side can be written as follows [10]:

$$v_{qs} = R_s i_{qs} + \frac{d\Psi_{qs}}{dt} + \omega_e \Psi_{ds} \quad (1)$$

$$v_{ds} = R_s i_{ds} + \frac{d\Psi_{ds}}{dt} - \omega_e \Psi_{qs} \quad (2)$$

and for the rotor side:

$$v_{qr} = R_r i_{qr} + \frac{d\Psi_{qr}}{dt} + (\omega_e - \omega_r)\Psi_{dr} \quad (3)$$

$$v_{dr} = R_r i_{dr} + \frac{d\Psi_{dr}}{dt} - (\omega_e - \omega_r)\Psi_{qr} \quad (4)$$

where:

v_{ds} , v_{qs} : d^e and q^e axes stator voltages respectively.

v_{dr} , v_{qr} : d^e and q^e axes rotor voltages respectively.

i_{ds} , i_{qs} : d^e and q^e axes stator currents respectively.

i_{dr} , i_{qr} : d^e and q^e axes rotor currents respectively.

Ψ_{ds} , Ψ_{qs} : d^e and q^e axes stator flux linkages respectively.

Ψ_{dr} , Ψ_{qr} : d^e and q^e axes rotor flux linkages respectively.

R_s , R_r : Stator and rotor resistances respectively.

ω_e : Stator or line frequency [rad/s].

ω_r : Rotor electrical speed.

For squirrel cage rotor IM, the rotor voltages v_{dr} and v_{qr} in Eqs. (3) and (4) are zero because the rotor circuit is short circuited.

The developed torque in the IM can be expressed in d-q axes stator variables in the synchronous reference frame by the following equation:

$$T_e = \frac{3}{2}\left(\frac{P}{2}\right)\left(\Psi_{ds} i_{qs} - \Psi_{qs} i_{ds}\right) \quad (5)$$

where P is the number of poles in the machine.

4.2. IM Drive Control

As noted before, the best control method for the IM is the FOC or vector control for its ability to imitate the separately excited DC motor's performance, where the motor torque can be controlled independently from motor flux and vice versa.

The block diagram of the FOC of the IM is shown in Fig. 5, which is based on the indirect FOC described in [10].

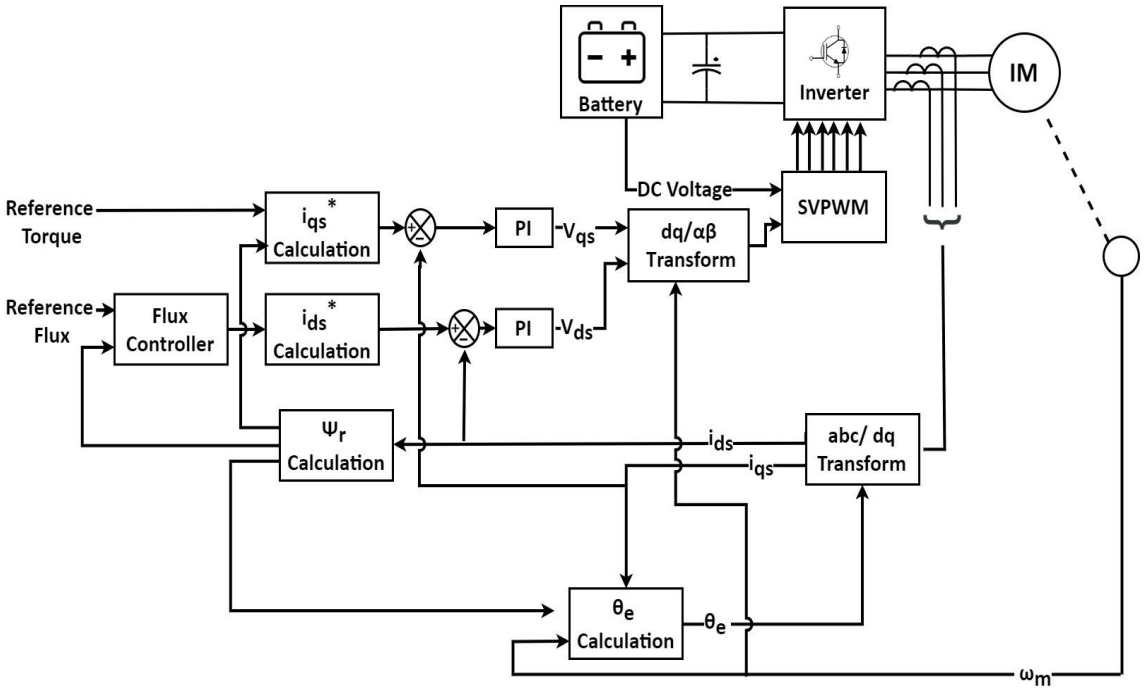

Fig. 5. Block diagram of the field oriented speed control of IM.

The flux vector Ψ_r calculation block calculates the flux Ψ_r using the equation:

$$\Psi_r = L_m i_{ds} \quad (6)$$

where L_m is the magnetizing inductance.

The i_{qs}^* calculation block calculates the quadrature current component reference value using the reference torque value and the flux vector Ψ_r value, which were calculated previously. The equation used in the block is:

$$i_q^* = \frac{2}{3}\left(\frac{2}{P}\right)\left(\frac{L_m}{L_r}\right)\left(\frac{T_e^*}{\Psi_r}\right) \quad (7)$$

The i_{ds}^* calculation block calculates the direct current component reference value using the flux vector Ψ_r reference value:

$$i_{ds}^* = \frac{\Psi_r^*}{L_m} \quad (8)$$

The angle of the synchronously rotating frame θ_e calculation block calculates the rotor flux angle using this equation:

$$\theta_e = \int \left[\left(\frac{P}{2}\ \omega_r\right) + \left(\frac{L_m R_r}{L_r \Psi_r}\ i_{qs}\right)\right] dt \quad (9)$$

which is based on this equation:

$$\theta_e = \int \omega_e\, dt = \int \omega_r + \omega_{sl}\, dt \quad (10)$$

where ω_{sl} is the slip speed.

The reference torque is generated from the speed controller, which is proportional to the speed command. The flux command is also generated using the speed command, but it has two regions: constant flux region which is under the rated speed; and the field-weakening region where the flux is inverse-proportional to the speed command.

5. IPMSM DRIVE

5.1. IPMSM Mathematical Model

The d-q model of the IPMSM is considered in the rotor reference frame, which rotates at the synchronous speed, because the angle of the instantaneous induced EMFs and consequently the angles of stator current and torque of the machine are determined by the position of the rotor's magnets. Considering the rotor reference frame transforms the d and q equivalent axis stator windings to the reference frame that revolves at the rotor speed, which makes zero differential speed between the rotor and stator's magnetic fields. It also stabilizes the relationship between stator d and q axis windings and rotor's magnet axis [18].

The equations of the d-axis and q-axis voltages are[10]:

$$v_{ds} = R_s i_{ds} - \omega_e \Psi_{qs} + \frac{d\Psi_{ds}}{dt} \quad (11)$$

$$v_{qs} = R_s i_{qs} + \omega_e \Psi_{ds} + \frac{d\Psi_{qs}}{dt} \quad (12)$$

where:

$$\Psi_{ds} = \Psi_f + i_{ds} L_{ds} \quad (13)$$

$$\Psi_{qs} = i_{qs} L_{qs} \quad (14)$$

and in terms of d-axis and q-axis currents [10]:

$$\frac{di_{ds}}{dt} = \frac{1}{L_{ds}} v_{ds} - \frac{R_s}{L_{ds}} i_{ds} + \frac{L_{qs}}{L_{ds}} \omega_e i_{qs} \quad (15)$$

$$\frac{di_{qs}}{dt} = \frac{1}{L_{qs}} v_{qs} - \frac{R_s}{L_{qs}} i_{qs} - \frac{L_{ds}}{L_{qs}} \omega_e i_{ds} - \frac{1}{L_{qs}} \omega_e \Psi_f \quad (16)$$

The developed torque in the machine is given by the following equation [10]:

$$T_e = 1.5p[\Psi_f i_{qs} + (L_{ds} - L_{qs}) i_{ds} i_{qs}] \quad (17)$$

where Ψ_f is the flux linkage of the permanent magnets.

5.2. IPMSM Drive Control

According to [19], the maximum torque per ampere control is the preferred control method to drive the IPMSM in the electric vehicles application, due to the high torque capability at low speeds and wide speed range, which are suitable for electric vehicle applications requirements.

The objective of maximum torque per ampere control method is to find the minimum current vector that achieves the required torque or the current vector that provides the maximum constant torque. This method is called maximum torque per ampere (MTPA) control [20].

There are many methodologies in the literature to derive the current formulas for the maximum torque per ampere operation. Simulink offers a MTPA current reference generator for the IPMSM control, which is based on the theory described in [19, 21, 22].

The current reference generator uses look-up tables that generate direct and quadrature currents commands using the torque command and motor speed values. These look-up tables are used instead of the online solving of the very complicated equations that achieve maximum torque per ampere criteria. These equations are described in [19, 21] . The block diagram of the MTPA-based drive for IPMSM is shown in Fig. 6.

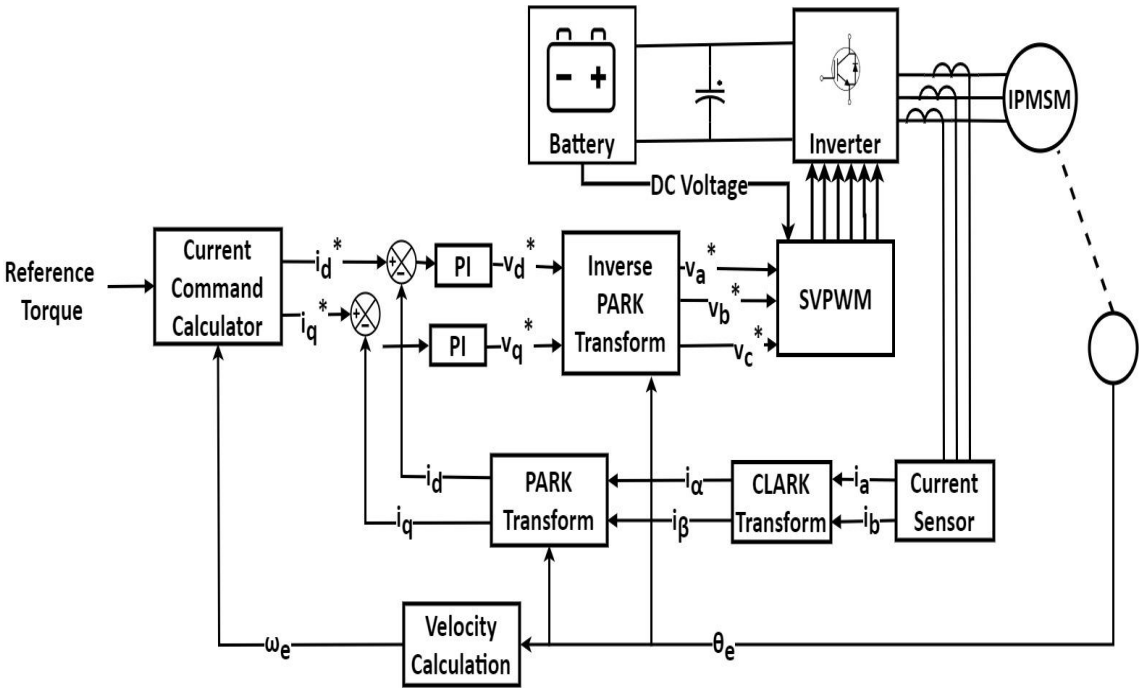

Fig. 6. Block diagram of the MTPA-based drive for IPMSM.

6. FUZZY LOGIC SPEED CONTROLLER

The motors' speed is controlled by a speed controller that generates the torque reference signal for the motor drive. The fuzzy logic control method has been chosen due to its superior performance over other methods, and not being affected by the variation of the system's parameters; it can be used with IM and IPMSM drives with the same parameters [10]. The block diagram of the fuzzy logic speed controller is

shown in Fig. 7. The speed reference is given to the controller through a speed ramps block, which increases and decreases the reference speed gradually for a stable operation. The actual speed is filtered through a low-pass filter for more stability.

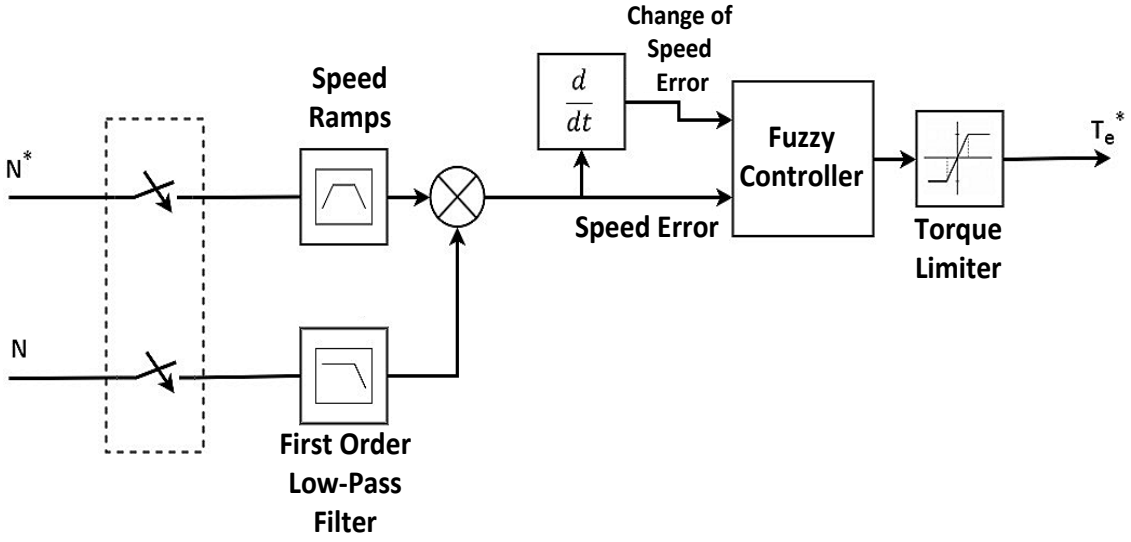

Fig. 7. Block diagram of the fuzzy logic speed controller.

The inputs of the fuzzy controllers are the speed error and the change of the speed error. The output torque reference is limited to the rated torque of the motors to keep the motors' current at rated values. The used membership functions of the speed error input, the change of the speed error input, and the output of the fuzzy logic controller are shown in Figs. 8-10, whereas the fuzzy rules matrix is shown in Table 6, in which E is the speed error; and CE is the change of speed error, whereas the rest constitutes the output of the fuzzy logic controller, namely, NB (Negative Big); NM (Negative Medium); NS (Negative Small); Z (Zero); PS (Positive Small); PM (Positive Medium); and PB (Positive Big).

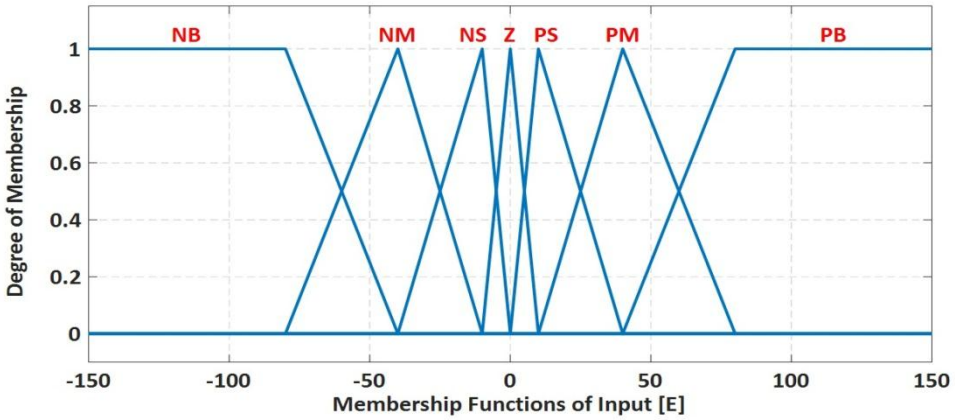

Fig. 8. Membership functions of the speed error input.

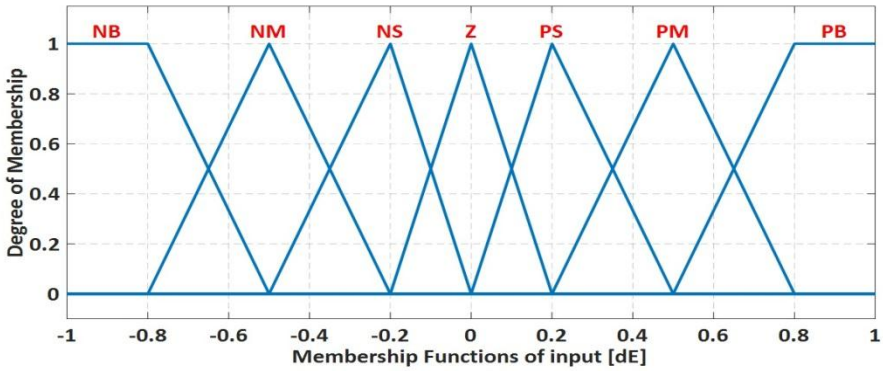

Fig. 9. Membership functions of the change of speed error input.

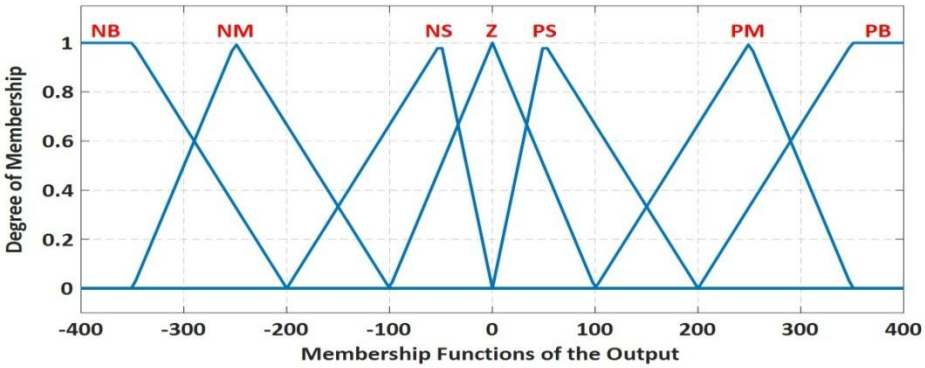

Fig. 10. Membership functions of the fuzzy logic controller output.

Table 6. Fuzzy rules matrix of the FLC speed controller.

E \ CE	NB	NM	NS	Z	PS	PM	PB
NB	NB	NB	NB	NB	NM	NS	Z
NM	NB	NB	NB	NM	NS	Z	PS
NS	NB	NB	NM	NS	Z	PS	PM
Z	NB	NM	Z	Z	Z	PM	PB
PS	NM	NS	Z	PS	PM	PB	PB
PM	NS	Z	PS	PM	PB	PB	PB
PB	Z	PS	PM	PB	PB	PB	PB

7. RESULTS AND DISCUSSION

To perform the comparison and to test the performance of both motors' drives, the motors were tested at no-load conditions and with vehicle body load conditions.

7.1. No Load Speed Response

The speed response, torque response, and output power of the IM with the FLC are demonstrated in Figs. 11-13. The figures show the operation of the motor in a constant torque region (below rated speed) and in a constant power region (above rated speed) where the torque starts to decrease after the speed exceeds the rated synchronous speed of 1800 rpm.

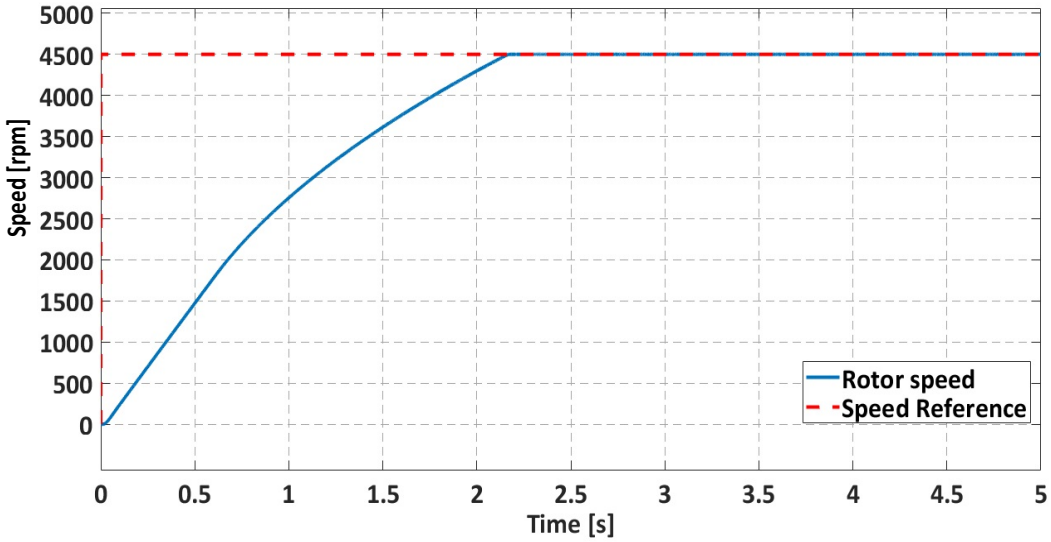

Fig. 11. IM speed response for 4500 rpm step speed command.

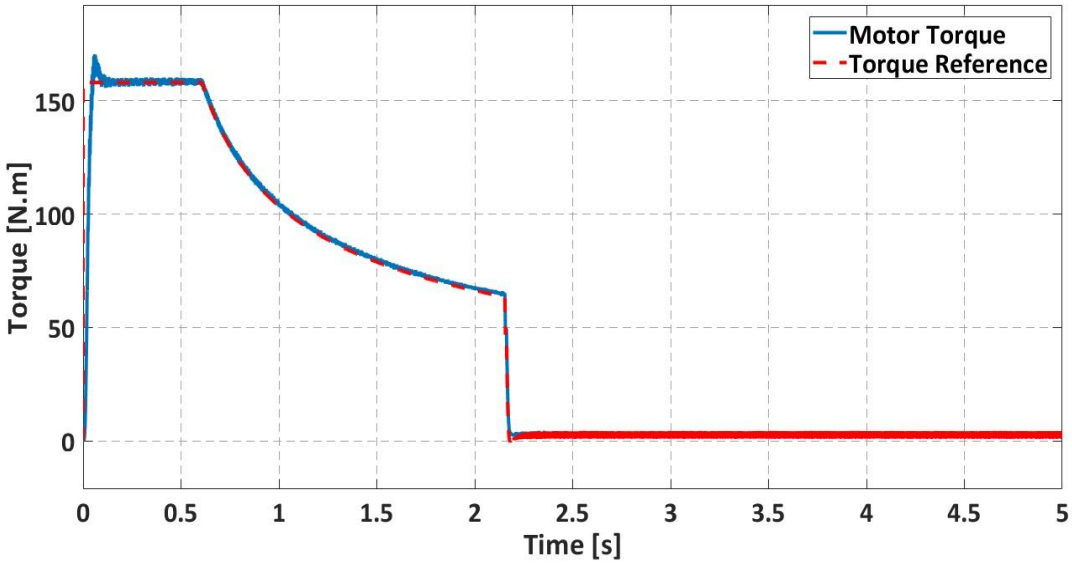

Fig. 12. IM torque response for 4500 rpm step speed command.

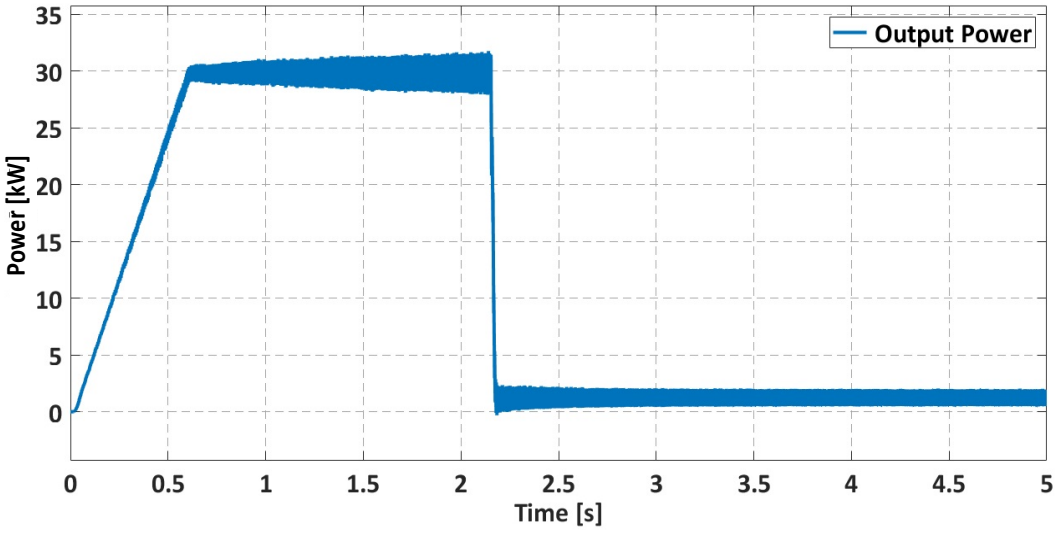

Fig. 13. IM output power for 4500 rpm step speed command.

Similar responses for the IPMSM are also shown in Figs. 14 -16. The operations of the IPMSM in a constant torque region and in a constant power region are also shown in the figures.

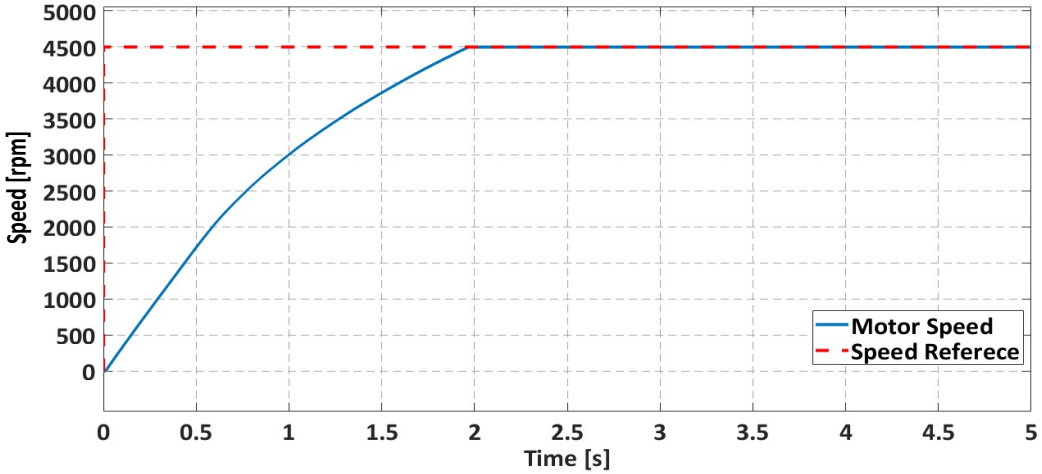

Fig. 14. IPMSM speed response for 4500 rpm step speed command.

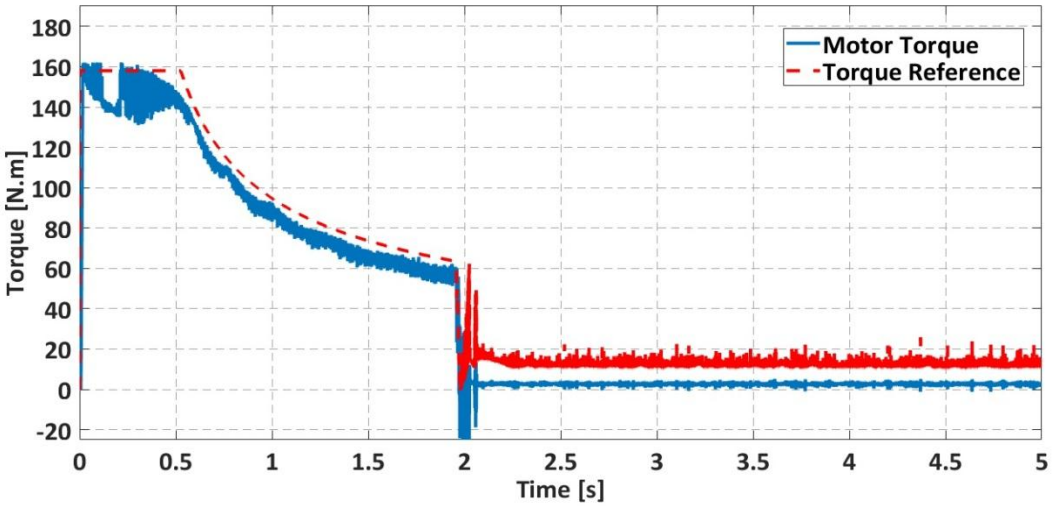

Fig. 15. IPMSM torque response for 4500 rpm step speed command.

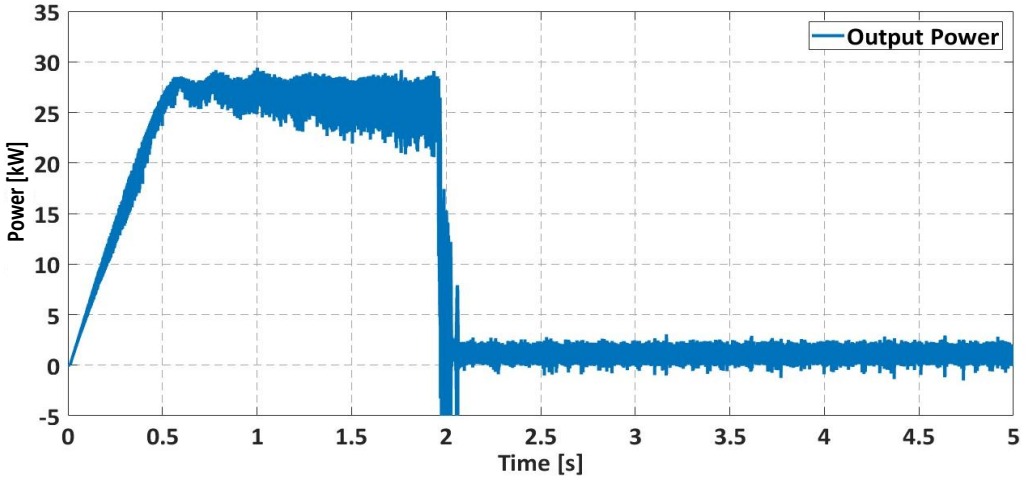

Fig. 16. IPMSM output power for 4500 rpm step speed command.

The characteristics of the speed response for both motors are shown in Table 7. The response of the IPMSM was faster than the IM in terms of rise time, settling time and peak time. On the other hand, the power output of the IPMSM is less than that in the IM, due to the high torque ripple of the IPMSM.

Table 7. Speed response characteristics with no load for IM and IPMSM drives with FLC speed controller.

Characteristic	IM drive	IPMSM drive
Speed reference [rpm]	4500	4500
Rise time [s]	1.6389	1.4914
Settling time [s]	2.0898	1.8959
Overshoot [%]	0	0.0012
Peak [rpm]	4500	4500.1
Peak Time [s]	2.1815	1.9800

7.2. Motors Response with Vehicle Body Load

In this part, the results of using the motors with the vehicle body model are discussed. The vehicle traction systems response is tested by a step speed response and by EUDC driving cycle.

7.2.1. Step Speed Vehicle Response

A 60 km/h speed command was given to both vehicles' drive systems. The speed response of the IM and the IPMSM-driven vehicles models are shown in Figs. 17 and 19, whereas their associated torque response is shown in Figs. 18 and 20. The characteristics of both responses are shown in Table 8.

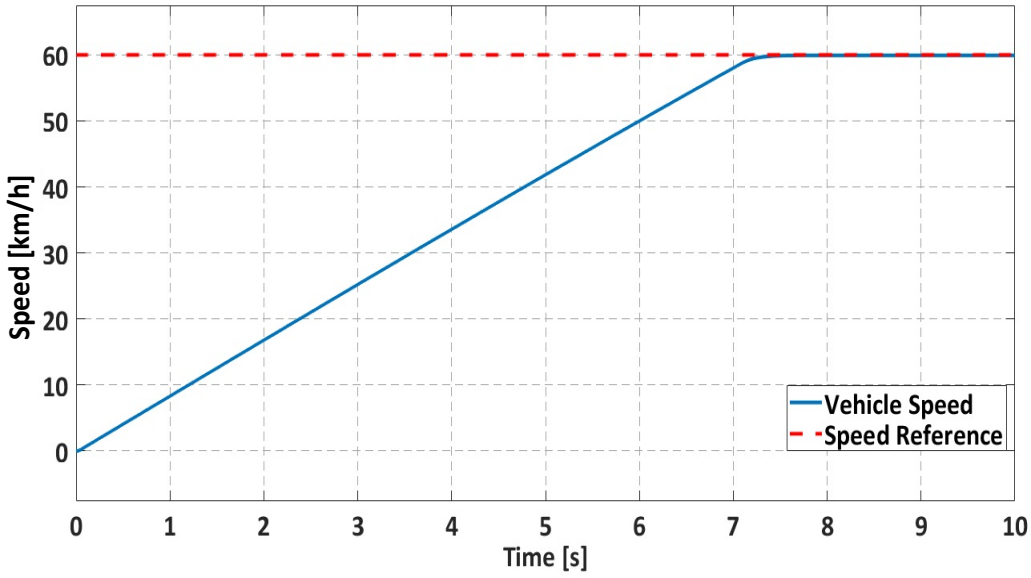

Fig. 17. Speed response of IM-driven electric vehicle.

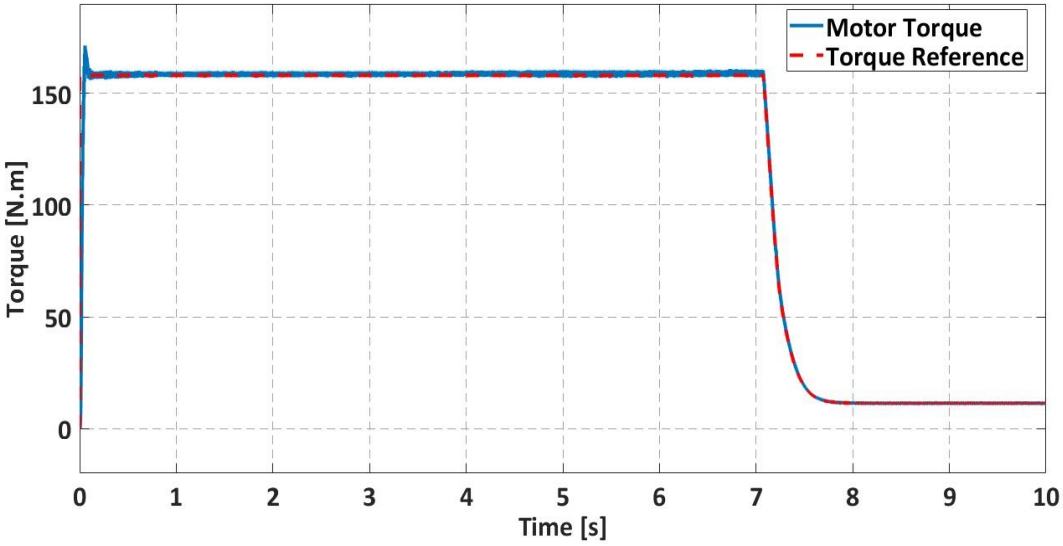

Fig. 18. Torque response of the IM-driven electric vehicle.

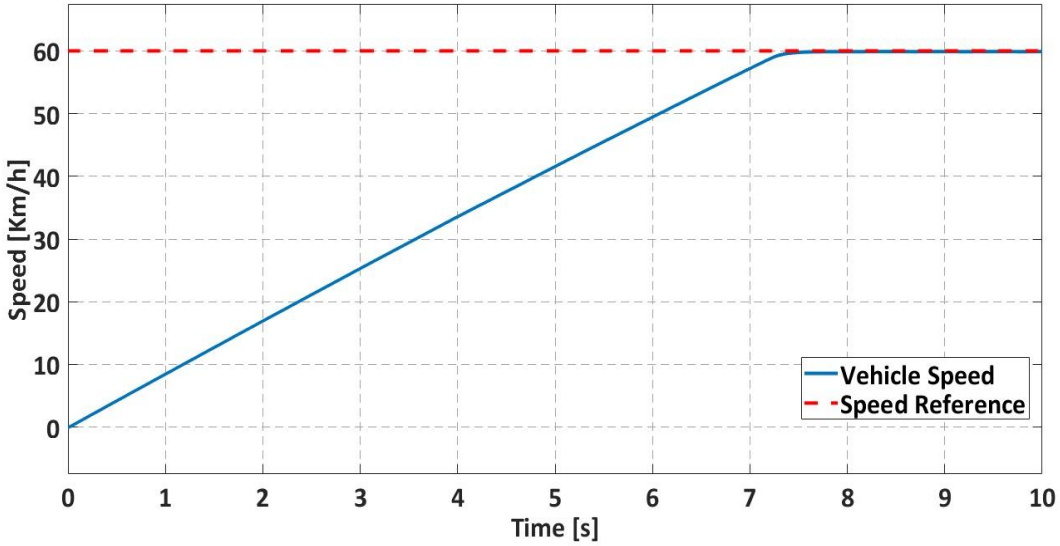

Fig. 19. Speed response of the IPMSM-driven electric vehicle.

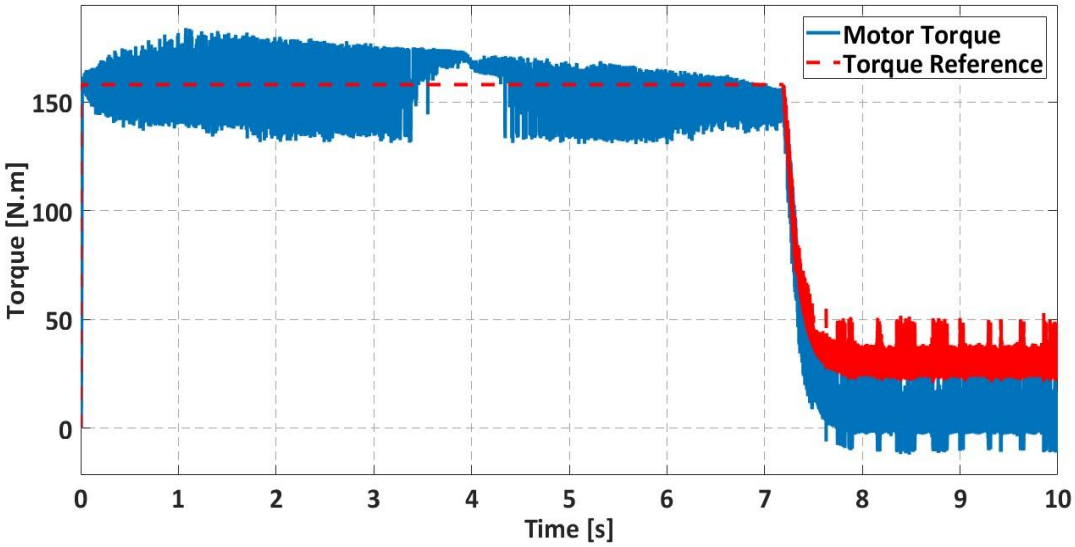

Fig. 20. Torque response of the IPMSM-driven electric vehicle.

According to Fig. 17 and 19 in addition to Table 8, there is no overshoot in both responses which is convenient to the electric vehicles applications. In comparison to the no-load conditions, the IM-driven vehicle model becomes faster than the IPMSM-driven model in terms of the rise and settling times; and this lag in the speed response of the IPMSM drive may be caused by the high torque ripple of the motor, which is shown in Fig. 20.

Table 8. Step speed response characteristics for IM and IPMSM driven vehicles.

Speed response characteristic	IM	IPMSM
Speed reference [km/h]	60	60
Rise time [s]	5.7666	5.8703
Settling time [s]	7.0964	7.2102
Overshoot [%]	0	0
Peak [rpm]	59.9346	59.8926
Peak time [s]	8.7650	8.4900

7.2.2. Driving Cycle Test

The driving cycle is a set of data points that define the vehicle's speed with respect to time, which is used to assess the performance of a vehicle in many aspects, usually fuel consumption and emissions. There are many driving cycles that are produced by many countries and organizations. The selected driving cycle is the EUDC, low power vehicles [23] as demonstrated in Fig. 21.

The performance of our models was tested by EUDC cycle to check the speed response in acceleration and deceleration states and in speed limiting performance.

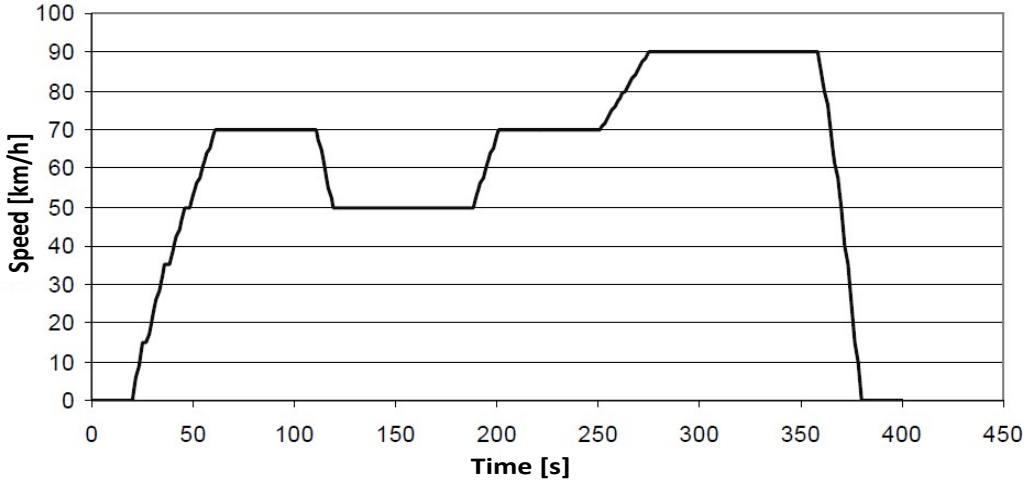

Fig. 21. Extra urban driving cycle, low power vehicles.

The performance of the IM-driven vehicle in the driving cycle - exhibited in Fig. 22 - shows that the vehicle speed response is completely in-line with the driving cycle speed reference.

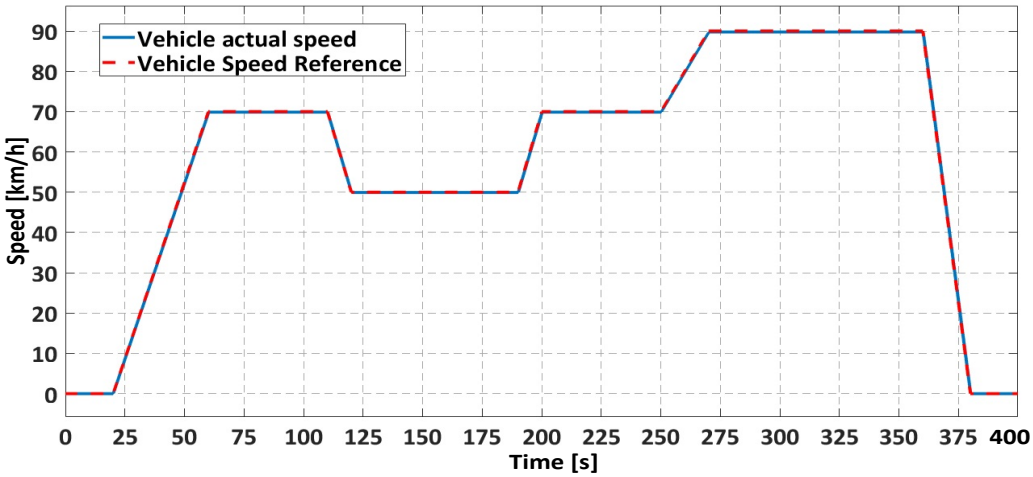

Fig. 22. Speed response of IM-driven for extra urban driving cycle, low power vehicles.

The torque response of the IM during the driving cycle is shown in Fig. 23. Also, the performance of the PMSM-driven vehicle is completely in-line with the driving cycle speed reference, as shown in Fig. 24 below. The torque response of the IPMSM during the driving cycle is shown in Fig. 25.

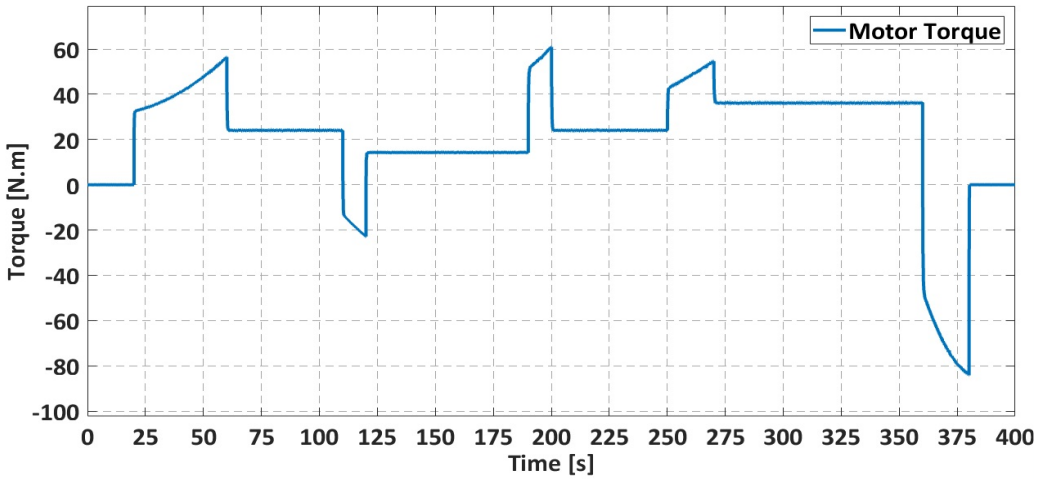

Fig. 23. Motor torque of the IM-driven electric vehicle.

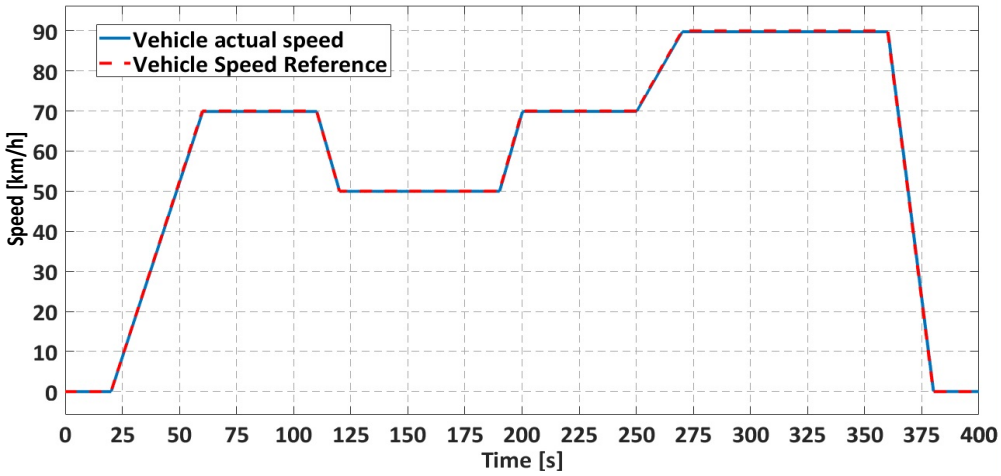

Fig. 24. Speed response of IPMSM-driven electric vehicle for low power extra urban driving cycle.

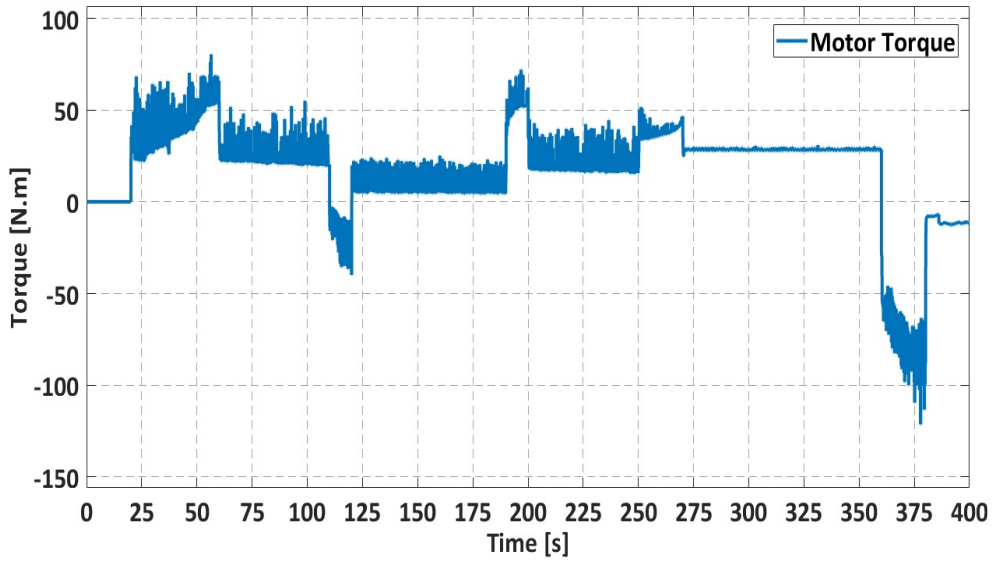

Fig. 25. Motor torque of the IPMSM-driven electric vehicle.

8. CONCLUSION

A dynamic comparison has been made between the IM and the IPMSM in electric vehicles applications using simulated models in Simulink software. The results of testing the motor drive models at no-load conditions and with vehicle body model and using EUDC driving cycle showed that the IPMSM drive has a little bit faster speed response in no-load test in comparison with the IM drive, but the latter was faster in the vehicle body load test. On the other hand, the IPMSM drive torque response showed more ripple than the IM. But in general the differences between them were minor specially that both models performed well in the EUDC driving cycle test.

Since the dynamic performance for both motors is relatively similar, other factors such as energy consumption, regenerative braking capability, the cost of each motor and the availability of the rare-earth magnets for the manufacturer may be considered when choosing between the IM and IPMSM.

REFERENCES

[1] L. Kumar, S. Jain, "Electric propulsion system for electric vehicular technology: a review," *Renewable and Sustainable Energy Reviews*, vol. 29, pp. 924–940, 2014.

[2] M. Kane, "Global sales december and 2018: 2 million plug-in electric cars sold," *InsideEVs*, 2019.

[3] M. Cheng, M. Tong, "Development status and trend of electric vehicles in China," *Chinese Journal of Electrical Engineering*, vol. 3, no. 2, pp. 1–13, 2017.

[4] *HAMACO Industries Corporation*, "IPM motor features and motor technology," 2019. <http://www.hamaco-ind.com/motor_technology/index.html>

[5] M. Yilmaz, "Limitations/capabilities of electric machine technologies and modeling approaches for electric motor design and analysis in plug-in electric vehicle applications," *Renewable and Sustainable Energy Reviews*, vol. 52, pp. 80–99, 2015.

[6] Y. Sato, S. Ishikawa, T. Okubo, M. Abe, K. Tamai, "Development of high response motor and inverter system for the Nissan LEAF electric vehicle," *SAE Technical Paper*, no. 2011-01-0350, 2011.

[7] S. Cash, O. Olatunbosun, "Fuzzy logic field-oriented control of an induction motor and a permanent magnet synchronous motor for hybrid/electric vehicle traction applications," *International Journal of Electric and Hybrid Vehicles*, vol. 9, no. 3, 2017.

[8] Y. Guan, Z. Zhu, I. Afinowi, J. Mipo, P. Farah, "Comparison between induction machine and interior permanent magnet machine for electric vehicle application," *2014 17th International Conference on Electrical Machines and Systems*, vol. 2, pp. 144–150, 2014.

[9] G. Pellegrino, A. Vagati, B. Boazzo, P. Guglielmi, "Comparison of induction and PM synchronous motor drives for EV application including design examples," *IEEE Transactions on Industry Applications*, vol. 48, no. 6, pp. 2322–2332, 2012.

[10] B. BOSE, *Modern Power Electronics and AC Drives*, 2002.

[11] WEG Group, *W22 Three-Phase Electric Motor Technical (NEMA Market)*, 2019.

[12] R. Natarajan, V. Misra, "Parameter estimation of induction motors using a spreadsheet program on a personal computer," *Electric Power Systems Research*, vol. 16, no. 2, pp. 157–164, 1989.

[13] Marathon Electric, *SyMAX® Quick Reference Guide*, 2013.

[14] J. Hayes, R. de Oliveira, S. Vaughan, M. Egan, "Simplified electric vehicle power train models and range estimation," *2011 IEEE Vehicle Power and Propulsion Conference*, pp. 1–5, 2011.

[15] M. Cavcar, "The international standard atmosphere," *Anadolu University*, pp. 1–7, 2000.

[16] A. Emadi, *Advanced Electric Drive Vehicles*, 2015.

[17] B. Tabbache, S. Djebarri, A. Kheloui, M. Benbouzid, "A power presizing methodology for electric vehicle traction motors," *International Review on Modelling and Simulations*, vol. 6, no. 1, pp. 29-32, 2013.

[18] R. Krishnan, *Electric Motor Drives: Modeling, Analysis, and Control*, Prentice Hall, 2001.

[19] N. Yang, G. Luo, W. Liu, K. Wang, "Interior permanent magnet synchronous motor control for electric vehicle using look-up table," *Proceedings of The 7th International Power Electronics and Motion Control Conference*, vol. 2, pp. 1015–1019, 2012.

[20] S. Kim, Y. Yoon, S. Sul, K. Ide, "Maximum torque per ampere (MTPA) control of an IPM machine based on signal injection considering inductance saturation," *IEEE Transactions on Power Electronics*, vol. 28, no. 1, pp. 488–497, 2012.

[21] S. Carpiuc, D. Patrascu, C. Lazar, "Optimal torque control of the interior permanent magnet synchronous machine," *2011 XXIII International Symposium on Information, Communication and Automation Technologies*, vol. 14, no. 2, pp. 80–88, 2011.

[22] M. Haque, L. Zhong, M. Rahman, "Improved trajectory control for an interior permanent magnet synchronous motor drive with extended operating limit," *Journal of Electrical and Electronics Engineering*, vol. 22, no. 1, p. 49-57, 2003.

[23] T. Barlow, S. Latham, I. McCrae, P. Boulter, "A reference book of driving cycles for use in the measurement of road vehicle emissions," *TRL Published Project Report*, 2009.